Radiative lifetime of excitons in ZnO nanocrystals: The dead-layer effect

Vladimir A. Fonoberov* and Alexander A. Balandin[†]

Nano-Device Laboratory,[‡] Department of Electrical Engineering, University of California-Riverside, Riverside, California 92521, USA

(Received 26 April 2004; published 11 November 2004)

We theoretically investigate exciton states of colloidal nearly spherical ZnO nanocrystals with diameters from 2 nm to 6 nm. The sizes of considered ZnO nanocrystals are chosen to be slightly larger than the exciton Bohr radius of bulk ZnO. A number of characteristic features of excitons are revealed in this intermediate quantum confinement regime. The exciton center of mass is found to be prolate along the c axis of wurtzite ZnO and squeezed to the center of the ZnO nanocrystal, thus forming a dead layer near the nanocrystal surface. The thickness of the exciton dead layer is found to increase with the nanocrystal size reaching the value of about 1.6 nm for the nanocrystal with diameter of 6 nm. Based on our calculations we proposed an analytical approximation for the exciton radiative-lifetime dependence on radius R in ZnO nanocrystal written as $\tau_0/[1+(R/R_0)^3]$ with $\tau_0 = 73.4$ ps and $R_0 = 2.55$ nm. Presented results and proposed analytical approximation can be used for interpretation of experimental data, and optimization of ZnO quantum dot structures for optoelectronic applications.

ZnO has recently attracted significant attention as a promising material for applications in ultraviolet light-emitting diodes, laser diodes, varistors, and transparent conducting films. Compared to other wide band-gap materials, ZnO has a very large exciton binding energy (~ 60 meV), which results in more efficient excitonic emission at room temperature. It is well known that semiconductor nanocrystals or quantum dots (QDs) may have superior optical properties than bulk crystals owing to quantum confinement effects.[1] For example, it has been experimentally established that the third-order nonlinear susceptibility of ZnO nanocrystals is ~ 500 larger that that of bulk ZnO.[2] A well-established fabrication technique, which utilizes colloidal suspension,[2–8] gives ZnO QDs of nearly spherical shape with diameters less than 10 nm. Thus, optical properties of colloidal ZnO QDs, such as exciton energy and radiative lifetime, are expected to be strongly affected by quantum confinement.

Interpretation of experimental data and optimization of ZnO QDs for optoelectronic device applications require a theoretical model for prediction of the energy and the oscillator strength of optical transitions. Due to specifics of wurtzite ZnO material system, such as degeneracy and anisotropy of the valence band as well as small dielectric constant and correspondingly strong electron-hole Coulomb interaction, simple one-band effective-mass models fail to give correct results. Recently, the tight-binding method has been used to compute the electron and hole states in ZnO QDs.[9] The electron-hole interaction in Ref. 9 has been taken into account by adding the exciton binding energy of $-1.8e^2/\varepsilon R$ (Ref. 10) to the energy of an electron-hole pair. However, Brus[11] has shown that the treatment of an exciton in ZnO QDs as an electron-hole pair is a rather poor approximation leading to significant errors. The pseudopotential model, which was shown to describe exciton states in a CdSe QD (Ref. 12) very well, to the best of our knowledge, has not been applied to ZnO quantum dots.

In this paper we focus on the properties of the lowest excitonic states in colloidal nearly spherical ZnO QDs with diameters in the range from 2 nm to 6 nm. Fonoberov *et al.*[13] have demonstrated that the multiband effective-mass model works surprisingly well for the description of lowest exciton states even for the quantum shells[14] as thin as one monolayer. Here, we employ this model, with some modifications, to calculate the lowest exciton states in ZnO QDs. In our numerical computations we use the effective-mass parameters listed in Ref. 15. Since the exciton Bohr radius a_B in bulk ZnO is about 0.9 nm,[15] the size of the considered QDs is from 2 to 3 times larger than the size of the bulk exciton. The latter results in a situation when the strength of the electron-hole Coulomb interaction and quantum confinement effects are comparable. Therefore, one cannot use either the "strong confinement" or "weak confinement" approximations[16] to obtain exciton states in such ZnO QDs. The strong confinement approximation ($R/a_B < \sim 2$) assumes that the electron and hole confinement energies are much larger than the Coulomb interaction energy and the electron and hole wave functions can be treated separately. The weak confinement limit ($R/a_B > \sim 4$) uses the assumption that Coulomb interaction is strong compared to quantum confinement and, as a result, the exciton wave function can be decomposed into the wave function of the exciton center of mass and the wave function of the relative electron-hole motion.

To determine excitonic states in ZnO QDs in the "intermediate confinement" regime, which is relevant to the reported experimental data and important for possible device applications, we solve the six-dimensional exciton problem. In the case of isotropic nondegenerate conduction and valence bands the aforementioned six-dimensional problem for spherical QDs can be reduced to a three-dimensional one with independent variables r_e, r_h, and θ', where θ' is the angle between the electron radius-vector $\mathbf{r}_e$ and hole radius-vector $\mathbf{r}_h$. However, the valence band of ZnO is degenerate and anisotropic. Therefore, we can only reduce the exciton

problem to a five-dimensional one by making use of the axial symmetry of exciton wave functions along the c axis of wurtzite ZnO. We calculate the exciton states using the following Hamiltonian:

$$\hat{H}_{\text{exc}} = [\hat{H}_e + V_{\text{s-a}}(\mathbf{r}_e)] - [\hat{H}_h - V_{\text{s-a}}(\mathbf{r}_h)] + V_{\text{int}}(\mathbf{r}_e, \mathbf{r}_h), \quad (1)$$

where the two-band electron and the six-band hole Hamiltonians $\hat{H}_e$ and $\hat{H}_h$ for wurtzite nanocrystals have been written explicitly in Ref. 17. Since dielectric constants in ZnO QD and the exterior medium are different the Coulomb potential energy of the electron-hole system in Eq. (1) is represented by the sum of the electron-hole interaction energy $V_{\text{int}}(\mathbf{r}_e, \mathbf{r}_h)$ and electron and hole self-interaction energies $V_{\text{s-a}}(\mathbf{r}_e)$ and $V_{\text{s-a}}(\mathbf{r}_h)$ defined in Refs. 11 and 18. Neglecting a very small spin-orbit splitting, which is about 10 meV (Refs. 19 and 20) for ZnO, we can simplify the exciton problem by using the one-band electron and the three-band hole Hamiltonians.

We choose the coordinate system in such a way that the z axis is parallel to the c axis of wurtzite ZnO. Due to the axial symmetry of the exciton problem, the z component of the exciton angular momentum M_z is a good quantum number. To compute the eigenstates of the Hamiltonian (1) we represent the three-component exciton envelope function in the following form:

$$\Psi_{M_z}(\mathbf{r}_e, \mathbf{r}_h)$$
$$= \frac{1}{2\pi} \sum_{m=-\infty}^{\infty} \begin{pmatrix} \Psi_{-1}^{M_z,m}(\rho_e, z_e; \rho_h, z_h) e^{i(m-1)\varphi} \times e^{i(M_z-1)\Phi} \\ \Psi_0^{M_z,m}(\rho_e, z_e; \rho_h, z_h) e^{im\varphi} \times e^{iM_z\Phi} \\ \Psi_1^{M_z,m}(\rho_e, z_e; \rho_h, z_h) e^{i(m+1)\varphi} \times e^{i(M_z+1)\Phi} \end{pmatrix},$$
$$(2)$$

where Ψ_{-1}, Ψ_0, and Ψ_1 are the components of exciton envelope function in front of the Bloch functions $|S[(X+iY)/\sqrt{2}]\rangle$, $|SZ\rangle$, and $|S[(X-iY)/\sqrt{2}]\rangle$, respectively. In Eq. (2) the angles φ and Φ describe the relative angular motion of the electron and the hole and their angular motion as a whole, correspondingly. Substitution of the wave function (2) into the envelope-function equation with Hamiltonian (1) gives the system of three five-dimensional differential equations with respect to functions $\Psi_\alpha^{M_z,m}(\rho_e, z_e; \rho_h, z_h)$. The obtained system is solved numerically using the finite-difference method. In the numerical calculation we have neglected the small penetration of the exciton wave function into the exterior medium.

To validate the model we calculated exciton ground state energy as a function of the QD radius for spherical ZnO QDs in water and compared it with experimental data reported in Refs. 4 and 5. As one can see in Fig. 1, our theoretical results are in excellent agreement with measurements. We have studied the influence of the QD shape and the exterior medium on the exciton ground state energy. Transmission electron microscopy (TEM) images of ZnO QDs show that a fraction of QDs are not spherical but rather prolate ellipsoids with the ratio of semiaxes of about 9/8.[5] Our calculations show that prolate ZnO QDs have smaller exciton ground state energy than spherical QDs with the same semiminor axis (shown by the dashed line in Fig. 1). If we consider ZnO
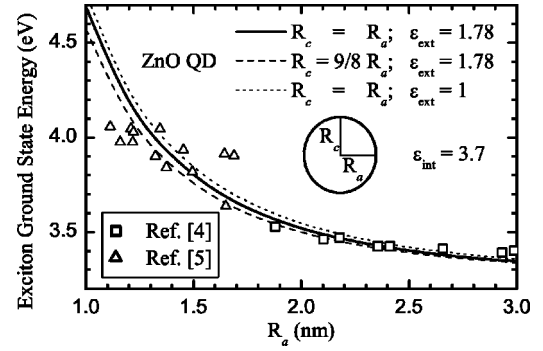

FIG. 1. Calculated exciton ground state energy in ZnO quantum dots as a function of the quantum dot radius (semiaxis) for spherical (ellipsoidal) quantum dots. Results are shown for two different ambient media: water ($\varepsilon = 1.78$) and air ($\varepsilon = 1$). For comparison we show experimental data points from Refs. 4 and 5.

QDs in air ($\varepsilon = 1$) instead of water ($\varepsilon = 1.78$), the exciton ground state energy increases (shown by the dotted line in Fig. 1). The difference in the ground state energies due to the change of the ambient (water→air) decreases from 70 meV to 13 meV when the QD radius increases from 1 nm to 3 nm. Overall it is seen from our calculations that small size dispersion of ZnO QDs and different exterior media have relatively small influence on the exciton ground state energy for the QDs with radius above 1.5 nm.

Interpretation of experimental data as well as prediction of the optical properties for ZnO QDs requires the knowledge of transition energies and their oscillator strength. The size dependence of the excited exciton states in spherical ZnO QDs is shown in Fig. 2. The energy of the excited states is counted from the exciton ground state energy. Figure 2 shows the size dependence of few lowest exciton states with $|M_z| = 0$, 1, 2. The oscillator strength f of an exciton state with energy E_{exc} and envelope wave function $\Psi_{\text{exc}}(\mathbf{r}_e, \mathbf{r}_h)$ is calculated as[17]

$$f = \frac{E_P}{E_{\text{exc}}} \left| \int_V \Psi_{\text{exc}}^{(\alpha)}(\mathbf{r}, \mathbf{r}) d\mathbf{r} \right|^2, \quad (3)$$

where the Kane energy of ZnO is $E_P = 28.2$ eV.[21] In Eq. (3) α denotes the component of the wave function, which is active
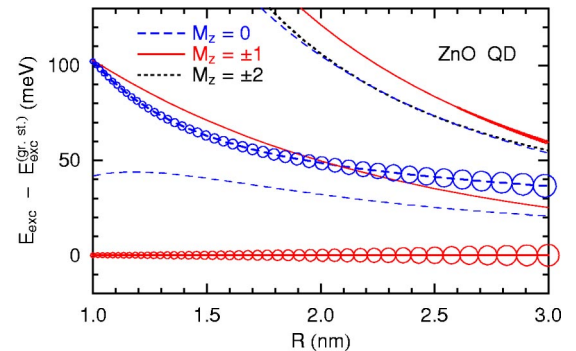

FIG. 2. (Color online) Energies of the excited exciton states (counted from the exciton ground state) as a function of the radius of spherical ZnO quantum dot in water. The oscillator strength of the corresponding transitions is depicted with circles. The size of the circles is proportional to the oscillator strength.

Exciton wave functions (center of mass)
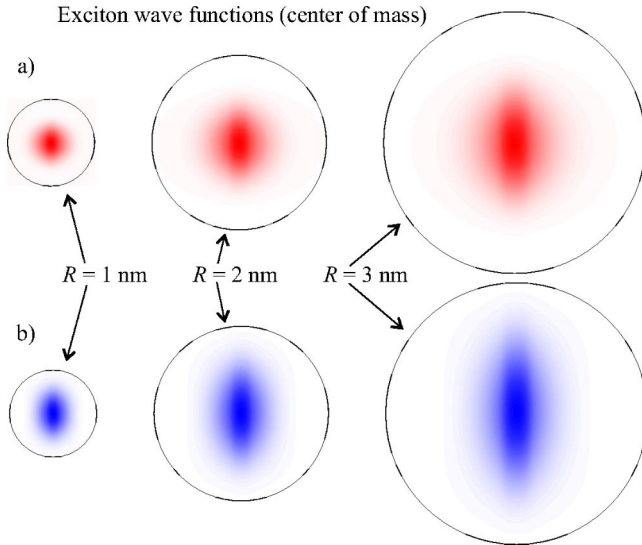
a)

b)

$R = 1$ nm $R = 2$ nm $R = 3$ nm

FIG. 3. (Color online) Optically active component of the exciton wave function (with equal electron and hole coordinates) of the first (a) and the second (b) bright exciton states for three different sizes of spherical ZnO quantum dots in water. The c axis of wurtzite ZnO is directed vertically.
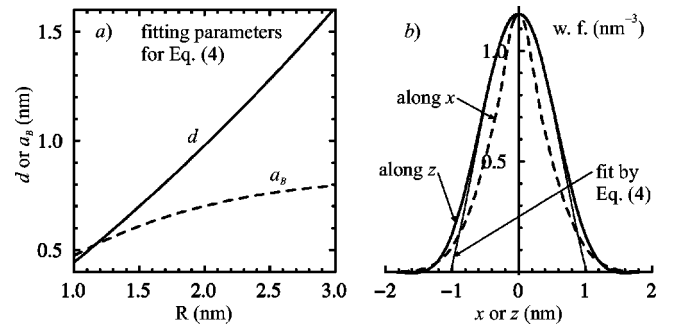

FIG. 4. (a) Fitting parameters for Eq. (4) as a function of ZnO QD radius; d is the dead layer thickness and a_B is the exciton Bohr radius. (b) Wave function of the exciton's center of mass along x and z axes for the 4 nm in diameter ZnO QD; thin solid line shows a fit by Eq. (4).

for a given polarization. In the dipole approximation, only exciton energy levels with $|M_z|=0, 1$ can be optically active, i.e., they can have a nonzero oscillator strength. Besides, the exciton energy levels with $M_z=0(M_z=\pm1)$ are optically active only for the polarization $\mathbf{e} \| \mathbf{z}(\mathbf{e} \perp \mathbf{z})$. The oscillator strengths of the corresponding exciton energy levels are depicted in Fig. 2 with circles. The size of the circles is proportional to the oscillator strength. We can see that there are two exciton levels that have large oscillator strengths. They are the first level with $|M_z|=1$, which is the exciton ground state, and the second level with $M_z=0$. The energy difference between the two exciton levels decreases while their oscillator strengths, which are almost the same for both levels, increase with increasing the QD size. Other exciton energy levels shown in Fig. 2 have zero or negligible oscillator strength.

Figure 3 shows the optically active component of the exciton wave function (with equal electron and hole coordinates) for each of the two brightest exciton states from Fig. 2 for QD radii 1 nm, 2 nm, and 3 nm. For QDs with $R>a_B$, the electron and hole motion around their center of mass prevents the center of mass from reaching the QD surface, thus, forming a so-called dead layer near the QD surface. The concept of the exciton dead layer can be traced back to Pekar.[22] It states that the exciton is totally reflected from an effective barrier located inside the QD at the distance d from the QD surface. To estimate the thickness d of the dead layer in ZnO QDs, we assume that only the optically active component of the exciton wave function is nonzero, what allows us to approximate the wave function of the exciton center of mass as

$$\Psi_{exc}(\mathbf{r},\mathbf{r}) = \frac{1}{\sqrt{\pi a_B^3}} \frac{\sin[\pi r/(R-d)]}{r\sqrt{2\pi(R-d)}}. \tag{4}$$

Assuming that Eq. (4) correctly reproduces the density of the exciton's center of mass, we can find the thickness d of the

dead layer and the exciton Bohr radius a_B from the following system:

$$\sqrt{\frac{8(R-d)^3}{\pi^2 a_B^3}} = \int_V \Psi_{exc}^{(\alpha)}(\mathbf{r},\mathbf{r})d\mathbf{r},$$

$$\frac{1}{\sqrt{2a_B^3(R-d)^3}} = \Psi_{exc}^{(\alpha)}(0,0). \tag{5}$$

Note that the system (5) is an identity when the optically active component $\Psi_{exc}^{(\alpha)}(\mathbf{r},\mathbf{r})$ of the wave function of exciton ground state is given by Eq. (4). The fitting parameters d and a_B found as solutions of system (5) are plotted in Fig. 4(a) as a function of the radius of ZnO QD in water. The quality of the fit is illustrated in Fig. 4(b) for the ZnO/water QD with $R=2$ nm. It is seen from Fig. 4(a) that the dead-layer thickness d increases almost linearly with R while the exciton Bohr radius tends to its bulk value (0.9 nm). Figure 3 confirms that the thickness of the dead layer increases with increasing the QD size. Our estimate gives the value of the dead-layer thickness $d=1.6$ nm for $R=3$ nm, which almost coincides with the dead-layer thickness calculated in Ref. 23 for a quantum well with thickness $L \gg a_B$ and $m_{hh}/m_e=9.5$.[15] The latter suggests that the thickness of the dead layer for larger ZnO QDs, i.e., in the weak confinement regime, is not noticeably larger than 1.6 nm. The relatively large thickness of the dead layer in colloidal ZnO QDs is attributed to the large ratio of hole and electron effective masses.

The fact that the exciton in the spherical ZnO QDs is prolate along the c axis (see Fig. 3) is attributed to the anisotropy of valence band of wurtzite ZnO. It is also seen from Fig. 3 that the exciton is more prolate for the second optically active state than it is for the first one. Figure 5 compares the distribution of an electron over the volume of the 4 nm in diameter ZnO QD with the distribution of the exciton's center of mass over the same volume. Keeping in mind that the conduction band of wurtzite ZnO is isotropic and the electron can occupy the entire volume of the QD (no dead layer), the characteristic features of the exciton in the ZnO QD are clearly seen. The exciton center of mass is prolate along the c axis of wurtzite ZnO and squeezed to the
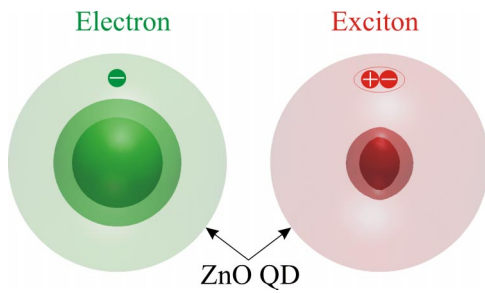
FIG. 5. (Color online) Distribution of the probability density of an electron and an exciton (center of mass) over the volume of the 4 nm in diameter spherical ZnO QD. The innermost and middle isosurfaces contain $1/3$ and $2/3$ of the total probability density, respectively.
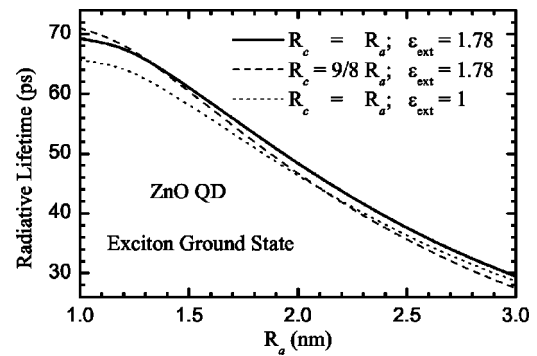

FIG. 6. Radiative lifetime of the exciton ground state in ZnO quantum dots as a function of the quantum dot radius (semiaxis) for spherical (ellipsoidal) quantum dots.

center of the ZnO QD. The above behavior of the exciton in a colloidal ZnO QD should strongly affect the exciton radiative lifetime.

The radiative recombination lifetime τ of excitons in bulk ZnO is about 322 ps,[24] which is small compared to other semiconductors. It is well known that the oscillator strength of localized excitons is substantially higher than that of free excitons.[25] Since the excitons are confined in ZnO QDs and the radiative lifetime $\tau = 2\pi\varepsilon_0 m_0 c^3 \hbar^2 / \sqrt{\varepsilon} e^2 E_{exc}^2 f$ (Refs. 17 and 26) is inversely proportional to the oscillator strength, one can expect for ZnO QDs very small exciton radiative lifetimes of the order of tens of picoseconds. To the best of our knowledge, no measurements of the exciton lifetime in ZnO QDs have been carried out. However, it has been established that the exciton lifetime is less than 50 ps for QDs with diameter 5 nm.[3]

The calculated radiative lifetime of the excitons in the ground state are shown in Fig. 6 as the function of the QD size. The solid line in Fig. 3 represents the radiative lifetime in the spherical ZnO QD in water, the dashed line shows the lifetime in the prolate ZnO QD in water, and the dotted line gives the lifetime in the spherical ZnO QD in air. For the QD with diameter 5 nm we get the lifetime of about 38 ps, in agreement with the conclusion of Ref. 3. We can see that the influence of the QD ellipticity and the exterior medium on the radiative lifetime in ZnO QDs is relatively weak. Analyzing the calculated dependence of the exciton lifetime on the radius of the spherical ZnO QD in water, we found that it can be fitted accurately with the function $\tau_0/[1+(R/R_0)^3]$,

where $\tau_0 = 73.4$ ps and $R_0 = 2.25$ nm. For larger QDs, i.e., in the weak confinement regime, the exciton lifetime is known to be inversely proportional to the QD volume.[26] Indeed, in this case substituting Eq. (4) into Eq. (3) one estimates $f \sim (R-d)^3/a_B^3$ and, therefore, $\tau \sim a_B^3/(R-d)^3$.

In conclusion, we used one-band electron–three-band hole envelope function model to calculate exciton states in colloidal ZnO QDs in the intermediate quantum confinement regime. The considered regime corresponds to the QD sizes, which are slightly larger than the size of an exciton in bulk ZnO. The exciton center of mass is found to be prolate along the c axis of wurtzite ZnO and squeezed to the center of the ZnO QD, thus forming a dead layer near the QD surface. Based on our calculations, we have predicted the size dependence of the exciton radiative lifetime in colloidal ZnO QDs. The presented results and proposed analytical approximation for the radiative lifetime can be used for interpretation of experimental data. The small radiative lifetime and rather thick dead layer in ZnO QDs are expected to be beneficial for optoelectronic device applications due to improved luminescence and exciton separation from the surface defects.

*Electronic mail: vladimir@ee.ucr.edu

†Electronic mail: alexb@ee.ucr.edu

‡Web address: http://ndl.ee.ucr.edu

[1] A. P. Alivisatos, Science **271**, 933 (1996).

[2] L. Guo, S. Yang, C. Yang, P. Yu, J. Wang, W. Ge, and G. K. L. Wong, Appl. Phys. Lett. **76**, 2901 (2000).

[3] D. W. Bahnemann, C. Kormann, and M. R. Hoffmann, J. Phys. Chem. **91**, 3789 (1987).

[4] E. A. Muelenkamp, J. Phys. Chem. B **102**, 5566 (1998).

[5] A. Wood, M. Giersig, M. Hilgendorff, A. Vilas-Campos, L. M. Liz-Marzan, and P. Mulvaney, Aust. J. Chem. **56**, 1051 (2003).

[6] E. M. Wong and P. C. Searson, Appl. Phys. Lett. **74**, 2939 (1999).

[7] H. Zhou, H. Alves, D. M. Hofmann, W. Kriegseis, B. K. Meyer, G. Kaczmarczyk, and A. Hoffmann, Appl. Phys. Lett. **80**, 210 (2002).

[8] A. Dijken, E. A. Muelenkamp, D. Vanmaekelbergh, and A. Meijerink, J. Phys. Chem. B **104**, 1715 (2000).

[9] R. Viswanatha, S. Sapra, B. Satpati, P. V. Satyam, B. N. Dev, and D. D. Sarma, J. Mater. Chem. **14**, 661 (2004).

[10] L. Brus, J. Phys. Chem. **90**, 2555 (1986).

[11] L. E. Brus, J. Chem. Phys. **80**, 4403 (1984).

[12] M. Califano, A. Zunger, and A. Franceschetti, Nano Lett. **4**, 525 (2004).

[13] V. A. Fonoberov, E. P. Pokatilov, V. M. Fomin, and J. T. Devreese, Phys. Rev. Lett. **92**, 127402 (2004).

[14] A. Mews, A. V. Kadavanich, U. Banin, and A. P. Alivisatos, Phys. Rev. B **53**, R13 242 (1996).

[15] The following parameters of wurtzite ZnO are taken from Ref. 19: electron effective mass $m_e = 0.24$; Rashba-Sheka-Pikus parameters of the valence band $A_1 = -3.78$, $A_2 = -0.44$, $A_3 = 3.45$, $A_4 = -1.63$, $A_5 = -1.68$, $A_6 = -2.23$, $A_7 = 0.47$ nm^{-1}; crystal-field splitting energy $\Delta_{cr} = 38$ meV; and dielectric constant $\varepsilon = 3.7$. The band-gap energy of wurtzite ZnO is $E_g = 3.437$ eV (Ref. 20). The heavy-hole effective mass can be estimated as $m_{hh} \approx 1/|A_2| = 2.27$, which gives the ratio $m_{hh}/m_e = 9.5$ in agreement with the tight-binding calculations (Ref. 27). Using the reduced exciton mass $\mu = m_e m_{hh}/(m_e + m_{hh})$, the exciton Bohr radius is estimated to be $a_B = 4\pi\varepsilon_0\hbar^2\varepsilon/e^2 m_0\mu = 0.90$ nm.

[16] Y. Kayanuma, Phys. Rev. B **38**, 9797 (1988).

[17] V. A. Fonoberov and A. A. Balandin, J. Appl. Phys. **94**, 7178 (2003).

[18] V. A. Fonoberov, E. P. Pokatilov, and A. A. Balandin, Phys. Rev. B **66**, 085310 (2002).

[19] W. R. L. Lambrecht, A. V. Rodina, S. Limpijumnong, B. Segall, and B. K. Meyer, Phys. Rev. B **65**, 075207 (2002).

[20] D. C. Reynolds, D. C. Look, B. Jogai, C. W. Litton, G. Cantwell, and W. C. Harsch, Phys. Rev. B **60**, 2340 (1999).

[21] P. Lawaetz, Phys. Rev. B **4**, 3460 (1971).

[22] S. I. Pekar, Sov. Phys. JETP **6**, 785 (1958).

[23] M. Combescot, R. Combescot, and B. Roulet, Eur. Phys. J. B **23**, 139 (2001).

[24] D. C. Reynolds, D. C. Look, B. Jogai, J. E. Hoelscher, R. E. Sherriff, M. T. Harris, and M. J. Callahan, J. Appl. Phys. **88**, 2152 (2000).

[25] E. I. Rashba and G. E. Gurgenishvili, Sov. Phys. Solid State **4**, 759 (1962).

[26] J. Bellessa, V. Voliotis, R. Grousson, X. L. Wang, M. Ogura, and H. Matsuhata, Phys. Rev. B **58**, 9933 (1998).

[27] A. Kobayashi, O. F. Sankey, S. M. Volz, and J. D. Dow, Phys. Rev. B **28**, 935 (1983).